A STUDY OF THE TRANSITION KINETICS FROM PARA-EQUILIBRIUM TO ORTHO-EQUILIBRIUM

John M. Vitek[1], Suresh S. Babu[1], and Ernst Kozeschnik[2,3]

[1] Oak Ridge National Laboratory, P. O. Box 2008, Oak Ridge, Tennessee, 37831-6096, USA
[2] Graz University of Technology, Kopernikusgasse 24/1, Graz A-8010, Austria
[3] Materials Center Leoben, Franz Josef Straße 13, 8700 Leoben, Austria

Abstract

The kinetics of austenite decomposition to ferrite in an Fe-3Mn-0.1C (wt %) alloy have been simulated using computational thermodynamics and diffusion-controlled kinetics models. The transformation was modeled for two different austenite-ferrite interface conditions: ortho-equilibrium or para-equilibrium followed by ortho-equilibrium. The ortho-equilibrium condition resulted in an extremely slow transformation rate. For the case of para-equilibrium followed by ortho-equilibrium, the first stage of the transformation rate was rapid (complete within a few hundred seconds) while the second stage was again slow. For the second case, the initial rapid ferrite formation was followed by transient ferrite dissolution and reformation once the ortho-equilibrium reaction was imposed. This behavior can be explained by considering the nature of the elemental fluxes at the interface. The predicted transformation behavior was also compared to expected behavior for a Local-Equilibrium-with-Negligible-Partitioning (LENP) condition. Preliminary results from experiments designed to critically evaluate the predictions are also presented and tend to support the para-equilibrium transformation mechanism.

Introduction

Austenite decomposition into ferrite in steels is of great interest, both from a commercial and theoretical point of view. Many various transformation mechanisms may occur, depending upon the thermal conditions and the alloy composition. Much research has been carried out over the years to identify the various mechanisms in an effort to be able to predict and control the microstructural evolution. Two mechanisms that have been proposed and investigated to describe the rapid formation of pro-eutectoid ferrite from a fully austenitic initial condition are Local-Equilibrium-with-Negligible-Partitioning (LENP) and Para-Equilibrium (PE). These two mechanisms have several similarities but they also have significant differences. A schematic diagram illustrating the principles behind these two proposed mechanisms is shown in Figure 1. In Figure 1a, an isothermal section (700°C) of the iron-rich corner of the Fe-Mn-C ternary phase diagram is depicted, with the phase boundaries and calculated tie-lines for both ortho-equilibrium and para-equilibrium conditions (FCC=austenite; BCC=ferrite; Fe_3C=cementite). In this paper, ortho-equilibrium is defined as equilibrium for all constituents whereas para-equilibrium is equilibrium for only the fast diffusing species (C), under the constraint that the slow diffusing components (Mn) are constant (and not in equilibrium). "Local equilibrium" simply indicates that equilibrium is imposed at the interface, under either ortho- or para-equilibrium conditions. LENP is a special case of ortho-equilibrium. Strictly speaking, LENP is local ortho-equilibrium with negligible partitioning, but it will be referred to as LENP to conform to convention used in the literature.

Figures 1b and 1c show schematic composition profiles at intermediate stages of the transformation of austenite to ferrite for the LENP and PE mechanisms, respectively. In the

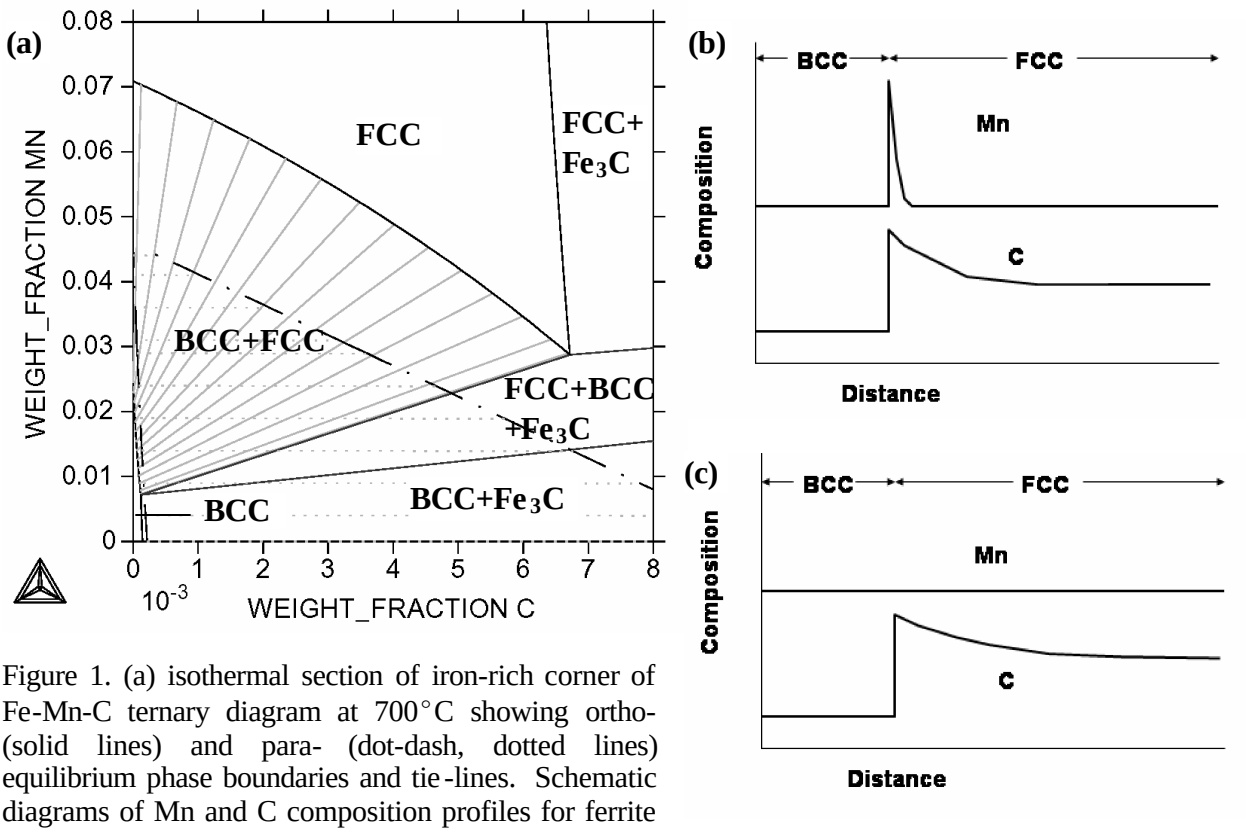

Figure 1. (a) isothermal section of iron-rich corner of Fe-Mn-C ternary diagram at 700°C showing ortho- (solid lines) and para- (dot-dash, dotted lines) equilibrium phase boundaries and tie-lines. Schematic diagrams of Mn and C composition profiles for ferrite growth under (b) LENP and (c) para-equilibrium conditions.

case of LENP, the interface between ferrite and austenite is in equilibrium, as given by an ortho-equilibrium tie-line in the phase diagram, with the added condition that the solute content of ferrite at the interface is equal to the solute content in the austenite far away fom the interface. This combination of conditions allows for rapid ferrite growth. In contrast, the PE case is based on the premise that at the interface there is no solute redistribution at all for slow moving substitutional species (Mn) whereas partitioning for rapidly diffusing interstitial species (C) is permitted so that the C potentials at the interface for both phases are equal. This condition leads to different tie-lines for PE, as shown in Figure 1a. For both mechanisms, C diffusion controls the transformation rate, and hence both mechanisms predict comparably fast ferrite growth kinetics. In addition, except for the steep spike in the substitutional solute concentration at the LENP interface, both mechanisms predict the ferrite product phase and parent austenite phases will have the same substitutional solute concentration. The differences between the two mechanisms include the appearance of a very sharp compositional spike at the interface for the LENP condition, and significantly different C concentrations at the growing interface. More details and examples of these two mechanisms may be found in the literature (see for example [1,2]).

In a broader sense, one may consider the transformation reactions, and their variation with increasing interface growth velocity, by examining the schematic diagram in Figure 2. This diagram shows the partition coefficient (defined as the concentration of the product phase divided by the concentration of the parent phase for the same element) for the slower diffusing substitutional solute atoms (Mn) on the ordinate and the partition coefficient for the rapidly diffusing interstitial atoms (C) on the abscissa. Two values are shown on each scale, the equilibrium partition coefficient, k_{eq}, and 1, representing partitionless transformation behavior. It is assumed that the equilibrium k's are less than 1 for convenience. Point A depicts the condition where partitioning for both rapid and slow diffusers is at the equilibrium level. This is the condition given by the equilibrium tie-lines in the phase diagram, and includes the

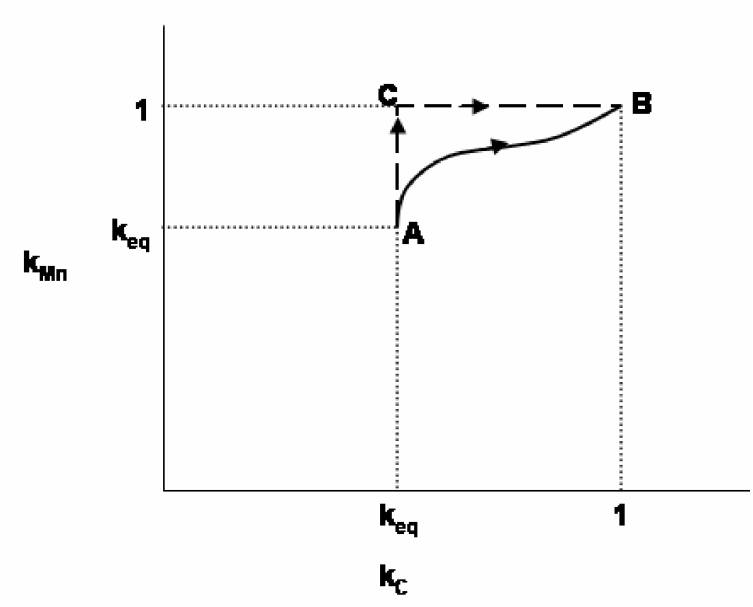

Figure 2. Schematic diagram of partition coefficient for interstitial (x-axis) and substitutional (y-axis) solutes for "A" ortho-equilibrium, "B" partitionless, and "C" para-equilibrium transformations. Arrows show behavior as growth velocity increases.

situation that exists under LENP. In contrast, point B represents no partitioning of either element, and this is the case under extremely rapid growth conditions where solute trapping prevents any elemental redistribution across the interface. The line which connects these two extremes describes the conditions at the interface when proceeding from a slow growth rate to a very rapid growth rate. The exact locus of the line is not known and is drawn by the arbitrary curvy line. If the diffusivities of the substitutional and interstitial elements are sufficiently far apart, it is plausible that at some intermediate growth rates partitioning of the slow diffusers will be completely prevented while partitioning of the rapid diffusers will be unimpaired. This is the condition at point C and represents the PE mechanism. In steels, where the diffusivities of the substitutional and interstitial species are orders of magnitude apart, the PE condition may be a reasonable approximation for a fairly wide range of transformation conditions and intermediate growth velocities. Thus, as the growth velocity of the transformation increases, the dashed arrow line may represent the changing interface conditions, going through the PE condition. It is the aim of this paper to describe simulation results for the formation of ferrite from austenite under such PE conditions, and to further explore the long-term transformation behavior when the PE condition changes to an ortho-equilibrium condition at the interface.

The Para-Equilibrium Phase Diagram For The Fe-Mn-C System

Computational thermodynamics has provided the means for calculating multi-component phase diagrams. In the same manner, para-equilibrium phase diagrams may be calculated under the additional compositional constraint of no substitutional solute element partitioning between phases [3]. Vertical sections of the ortho-equilibrium and para-equilibrium phase diagrams for the Fe-3%Mn-C system (all wt %) have been calculated and they are superimposed in Figure 3. The calculations were made using the ThermoCalc [4] and MatCalc [5] software packages and the SSOL database [6]. There are several unique sections in the diagram, where the predicted transformation behavior under ortho-equilibrium conditions is quite different from that under para-equilibrium conditions. These are shown by the numbered points. If one started in the austenite (γ) phase field and quenched down to position #1, ortho-equilibrium predicts austenite will partially transform to ferrite (α) whereas para-equilibrium predicts austenite will transform completely, to a combination of ferrite and cementite (Fe_3C). If a composition corresponding to point #2 is selected, quenching from the austenite phase field to point #2 would result in the formation of ferrite and cementite, yielding a three-phase microstructure, under ortho-equilibrium conditions while para-equilibrium predicts complete transformation of austenite to ferrite + cementite. In the present paper, a composition comparable to point #3 will be considered. The transformation of a fully austenitic microstructure to a ferrite + austenite microstructure is predicted for both ortho- and para-equilibrium conditions. However, the C

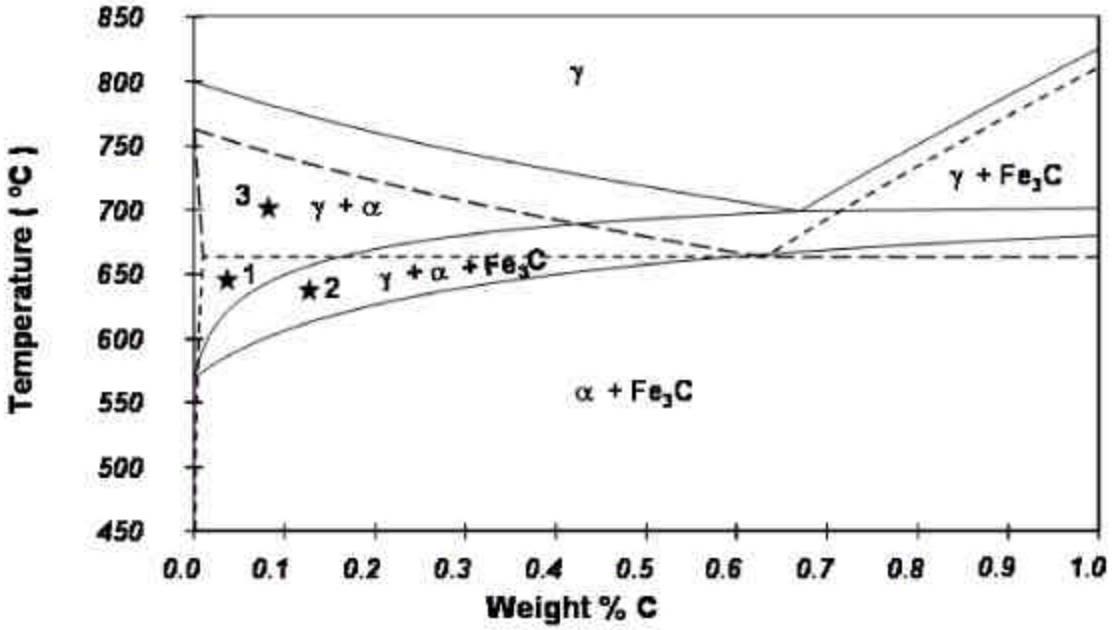

Figure 3. Superimposed ortho- and para-equilibrium vertical sections of the phase diagram for Fe-Mn-C. Numbered points represent special conditions described in the text.

concentrations of the phases differ, as well as the relative amounts of each phase.

Simulation Conditions

The alloy composition that is considered is Fe-3Mn-0.1C (wt%). The initial condition is a fully austenitic state, with uniform composition. The transformation to a two-phase ferrite + austenite microstructure at 700°C is simulated. A planar geometry (1-D) is used in the simulations, and the cell size is fixed at 25 μm. The composition and temperature correspond to point #3 in Figure 3. Two different simulation sequences were evaluated. The first (Case I), using the DiCTra software [7], imposes an ortho-equilibrium condition at the growing ferrite/austenite interface. Under this condition, partitioning of both Mn and C is allowed at the interface. This partitioning drives the diffusion process and the ferrite growth. The interface compositions are selected from the equilibrium tie-lines in such a way that the interface growth velocities due to the net Mn and C fluxes at the interface are equal. The second case considered a para-equilibrium condition at the

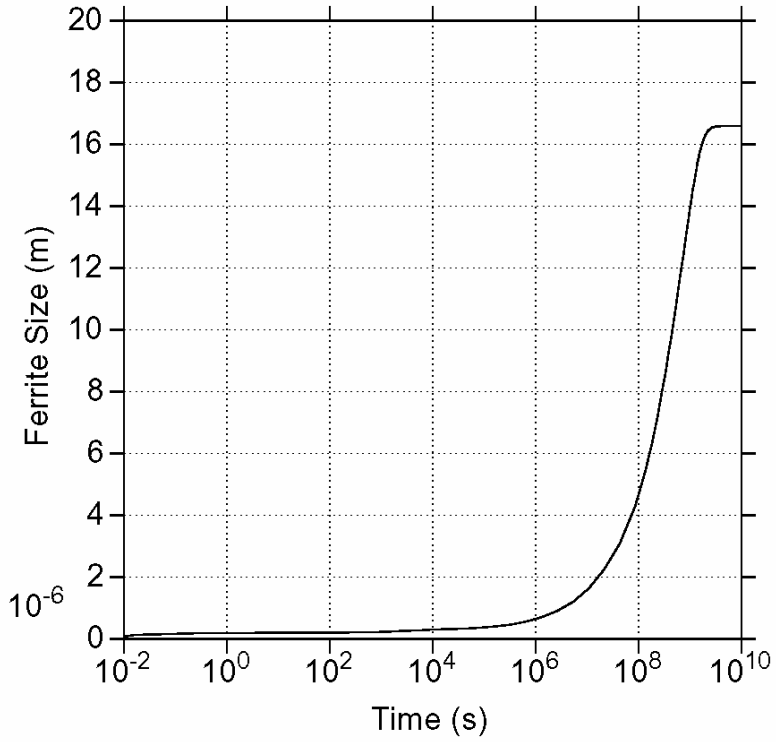

Figure 4. Simulation results showing ferrite size versus time for transformation under ortho-equilibrium interface conditions.

moving interface at the start of the simulation. Since the para-equilibrium phase diagram is comparable to a binary diagram, only one tie-line is available to describe the ferrite/austenite interface composition. When the para-equilibrium simulation reached completion (700 s), the simulation was continued by using the para-equilibrium state as the initial condition for an ortho-equilibrium simulation. In this way, the transition from para-equilibrium to ortho-equilibrium could be simulated, with the final state being the same as in the first, ortho-equilibrium only, case.

Ortho-Equilibrium (Case I) Simulation Results

The results from the ortho-equilibrium simulation are shown in Figure 4, where the ferrite size is plotted as a function of time. It can be seen that the transformation reaction is quite slow, with no appreciable ferrite formation taking place until approximately 10^5 s (30 h). The reaction is complete after approximately 3 x 10^9 s (over 30 years), with the final ferrite size equal to 16.6 μm (or 66 volume % ferrite). Plots of the composition profiles at selected times are shown in Figure 5. It is clear that Mn partitioning at the interface and Mn diffusion in austenite are controlling the reaction rate. Carbon diffusion is fast, leading to an essentially uniform C potential, but gradients in the C concentration exist. This is because the chemical potential of C is affected by the manganese concentration and its long-range gradient.

Para-Equilibrium Followed By Ortho-Equilibrium (Case II) Simulation Results

Similar to Figure 4, the results of the para- plus ortho-equilibrium simulation are shown in Figure 6 as ferrite size versus time. Several differences are found when compared to Figure 4. First, the para-equilibrium reaction is significantly faster. Therefore, appreciable ferrite forms after only seconds, and the para-equilibrium transformation is complete in less than 10^3 s (< 0.5 h). The subsequent imposition of ortho-equilibrium conditions at the interface (after 700 s) does not have any appreciable effect until after approximately 10^4 s. At that time, reversion of ferrite is predicted, followed by ferrite growth at a much later stage. Whereas the ferrite size reaches 18 μm (72 vol %) after para-equilibrium transformation, it reverts to a minimum of approximately 13 μm (52 vol %) before ultimately reaching the final equilibrium level of 16.6 μm (66 vol %). A representative composition profile confirming the para-equilibrium nature of

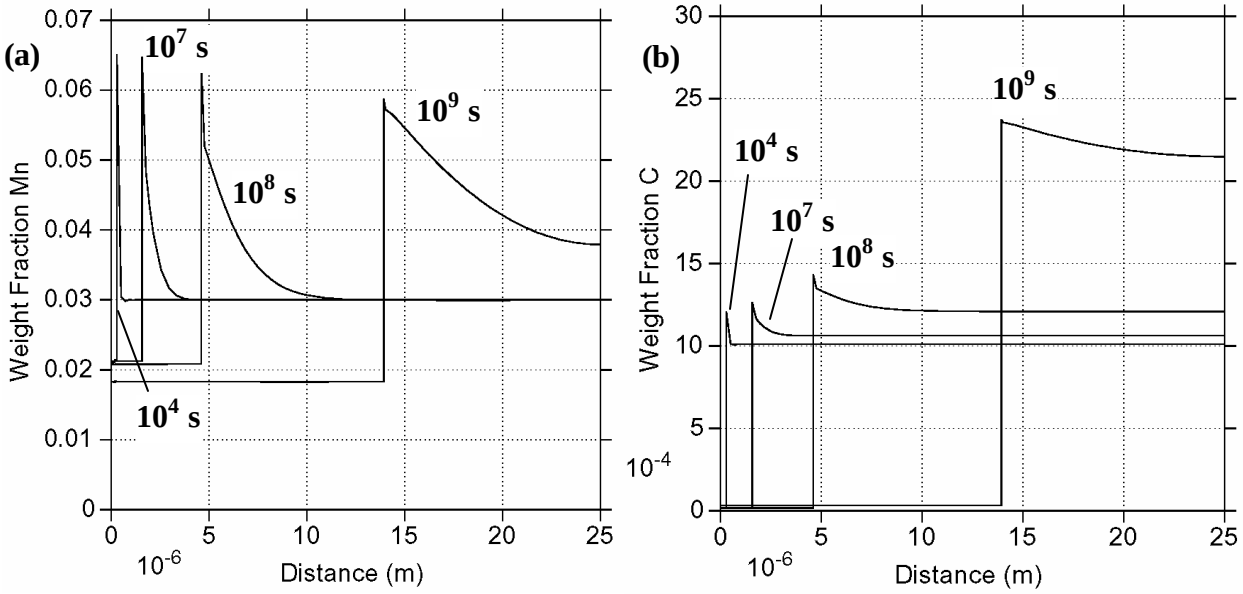

Figure 5. (a) Mn and (b) C concentration profiles at selected times during simulation under ortho-equilibrium interface conditions. Austenite is to right of interface, ferrite to left.

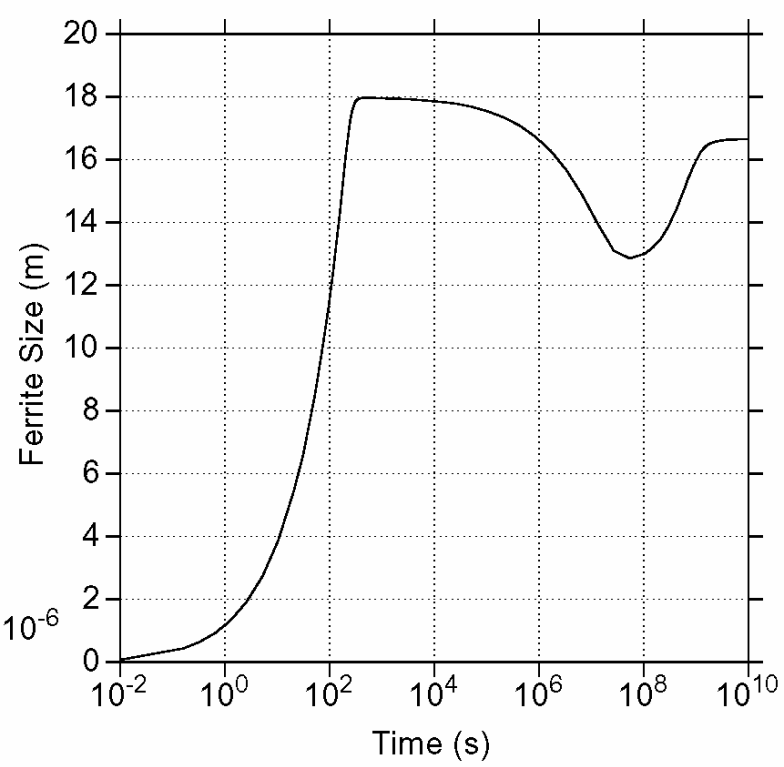

Figure 6. Simulation results showing ferrite size versus time for transformation with para-equilibrium condition at onset followed by ortho-equilibrium after 700s.

the simulation in the first stage is shown in Figure 7. The Mn concentration is uniform across both phases whereas the C level varies. The Mn concentration profiles during the latter ortho-equilibrium stage in Case II are shown in Figure 8. After short times (solid line; 10^4 s), comparable Mn gradients exist in both the ferrite and austenite phases at the interface. The Mn gradients in ferrite and austenite remain comparable during ferrite reversion (dashed line; 10^6 s). Near the minimum in ferrite size, and thereafter, the Mn gradients in the ferrite disappear whereas the gradients persist in the austenite (dot-dash and dotted lines; 5 x 10^7 and 10^9 s, respectively).

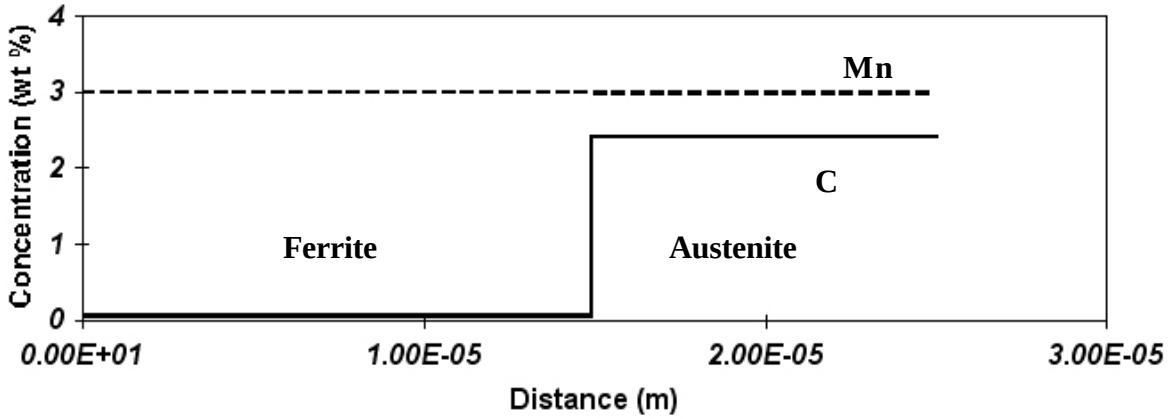

Figure 7. Mn and C concentration profiles at 199 s, during the para-equilibrium stage of the transformation simulation, showing uniform Mn profile and C partitioning.

Discussion

The results show that the austenite to ferrite transformation is exceedingly slow under ortho-equilibrium conditions whereas it is quite fast if para-equilibrium conditions are imposed on the interface. This is not surprising because in the former case, the slow Mn diffusion is controlling the reaction rate while in the latter, rapid C diffusion control of the transformation allows for much faster ferrite growth. However, the simulation results do show a rather unexpected feature, namely that as a result of the transition from para- to ortho-equilibrium conditions at the interface, a significant transient reduction in ferrite content is predicted. Thus, when changing from the para-equilibrium ferrite growth stage to the ortho-equilibrium growth stage, a monotonic change in ferrite size does not take place. The explanation for this unusual

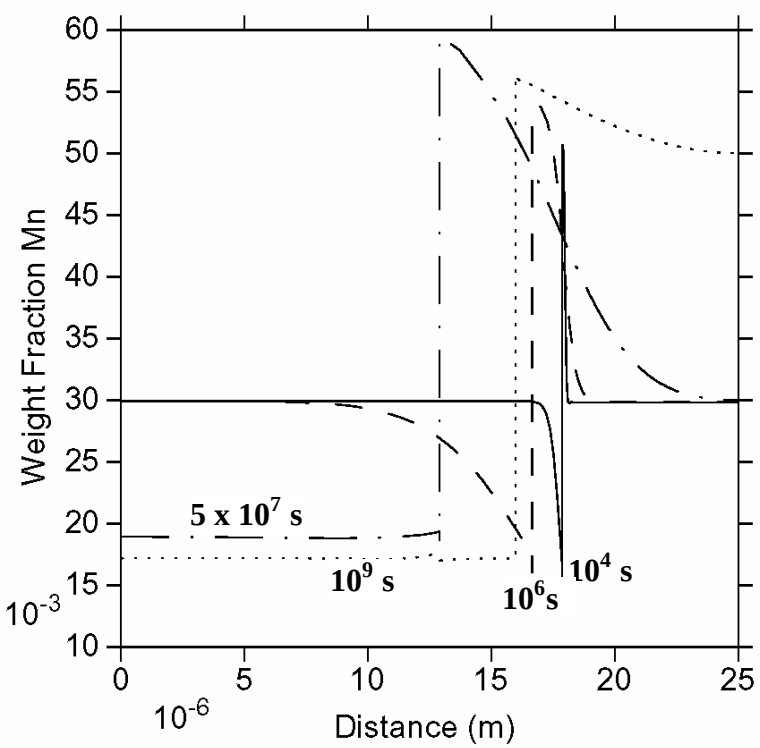

Figure 8. Mn concentration profiles during ortho-equilibrium stage of transformation simulation, following para-equilibrium stage. Various times correspond to different critical stages of transformation – see Figure 6. Austenite is to right of interface, ferrite to left.

behavior can be found by examining the Mn composition profiles in Figure 8. Once ortho-equilibrium is imposed at the ferrite/austenite interface, gradients are established in the Mn concentration in both the ferrite and austenite phases. The flux of Mn at the interface is the product of this gradient and the appropriate diffusion constants. Since the diffusion constant in ferrite is roughly two orders of magnitude greater than that in austenite, for comparable concentration gradients the flux in the ferrite will overwhelm the flux in the austenite. Since the flux of Mn in ferrite is toward the interface, austenite, with the higher Mn concentration, will grow at the expense of ferrite. At significantly later times, when the Mn gradients in the ferrite are flat while the gradients in the austenite are still present, the austenite flux will control the transformation behavior. Since the flux of Mn in austenite at the interface is away from the interface, a reversal will take place and the Mn-poor ferrite will grow again.

The relative amounts of ferrite and austenite after para-equilibrium may be greater or smaller than those after ortho-equilibrium, depending upon the alloy composition and the temperature. However, the initial shrinking of ferrite after switching from para-equilibrium to ortho-equilibrium at the interface may be a common feature, regardless of the composition. This may be understood by examining the isothermal section of the phase diagram that is shown in Figure1. The figure shows that the ortho-equilibrium tie-lines extend to lower Mn contents in the ferrite than in the overall alloy, and consequently, lower than the Mn content under para-equilibrium conditions. This means that during the switch from para- to ortho-equilibrium conditions at the interface, a flux of Mn toward the interface will always result. This is likely to be significantly greater than any flux of Mn away from the interface on the austenite side, leading to a growth of austenite and reversion of ferrite.

The transition from para-equilibrium to ortho-equilibrium can be compared to the behavior under LENP conditions, where a rapid first stage of transformation, in which the solute content is basically uniform and equal in the parent and product phases, is followed by the slower transition to final equilibrium. Simulations for both the Fe-Si-C and Fe-Mn-C systems show the transition is not accompanied by any reversion of ferrite [2]. This is because the LENP condition sets up a very steep gradient in the parent austenite phase. After LENP, as final equilibrium is approached, the flux of solute on the parent side is significantly greater than the opposing flux on the ferrite side, even though the diffusion coefficients in ferrite are much larger than in austenite. This is shown in Figure 9, for the case of ferrite growth from austenite in an Fe-1.5Mn-0.1C alloy at 700°C.

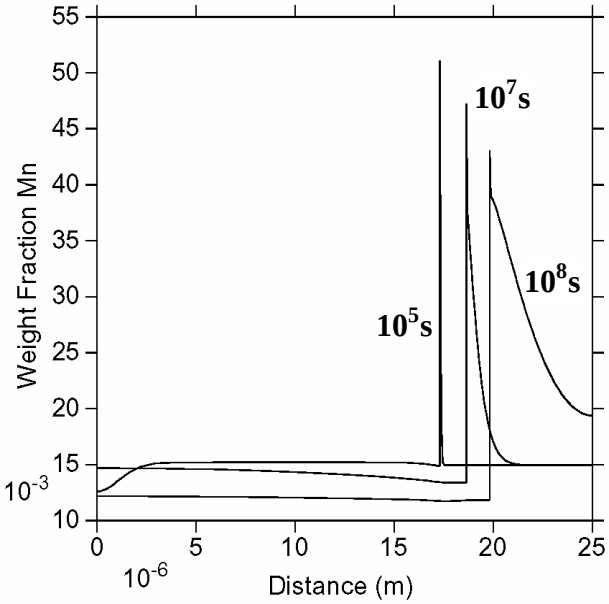

Figure 9. Results for a different alloy (Fe-1.5Mn-0.1C) which undergoes LENP at 700°C. Ortho-equilibrium transformation stage following LENP stage, showing limited Mn gradient in ferrite versus austenite. Austenite is on right.

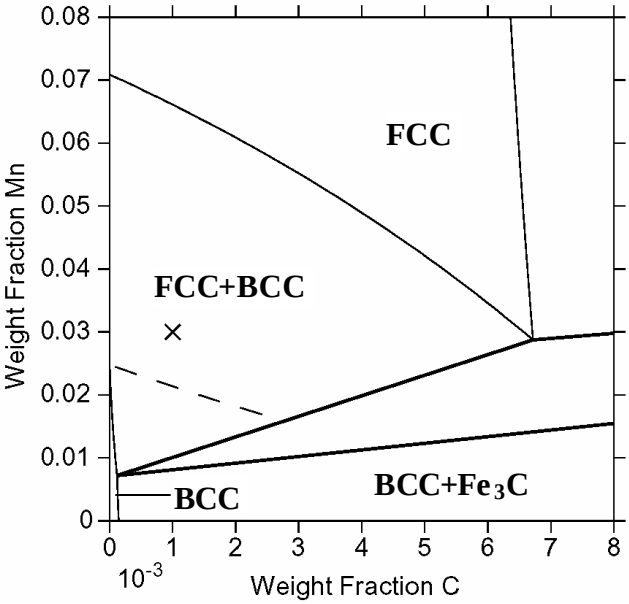

Figure 10. Isothermal section of iron-rich corner of Fe-Mn-C ternary diagram at 700°C showing LENP upper limit (dashed line) and composition ("X") of experimental alloy, which lies outside limit.

Experimental Studies

Experimental work is underway to determine whether the transformation of austenite to ferrite proceeds via a para-equilibrium mechanism during the early stages. The aim of this experimental phase is to distinguish between a PE transformation mechanism and an LENP mechanism. This is to be accomplished by two means. First, an alloy has been chosen that lies outside the LENP range. Such an LENP range can be defined by the condition that a tie-line with the same solute content as in the overall alloy can be drawn and, at the same time, the overall composition must establish a flux of C away from the interface within the parent austenite [2]. An isothermal section of the Fe-Mn-C ternary system at 700°C is shown in Figure 10, and the range of compositions in which LENP can occur is below the dashed line. The LENP limit is determined by the compositions where a tie-line can be drawn such that the product phase (ferrite) can have the same Mn composition as the overall alloy and the C activity (roughly the C concentration) in the parent phase (austenite) given by the tie-line is greater than the value for the overall alloy composition. The experimental alloy that has been chosen is an Fe-3Mn-0.1C alloy, shown by the "x" in Figure 10. This composition lies outside the LENP range. Thus, if rapid ferrite formation is found in this alloy, LENP must be excluded as a possible mechanism for this behavior. In contrast, rapid transformation could be explained by a para-equilibrium mechanism since this alloy lies within the two-phase para-equilibrium region (see Figure 1). The second feature that will investigated is whether there is any evidence of ferrite reversion after initial rapid ferrite formation. Such reversion is predicted in the para- plus ortho-equilibrium simulations and its existence would be strong evidence that the para-equilibrium transformation does in fact take place.

Very preliminary results from the experimental work are shown in Figure 11. An Fe-3Mn-0.1C alloy was austenitized and then quenched to 700°C and held for 2000 s. The dilation was measured as a function of time and the relative change in sample radius versus time is shown in the figure. There is evidence that a partial transformation takes place and reaches completion within the first 30 minutes. This is comparable to the time frame expected for transformation under para-equilibrium conditions. The rapid transformation cannot be explained by LENP

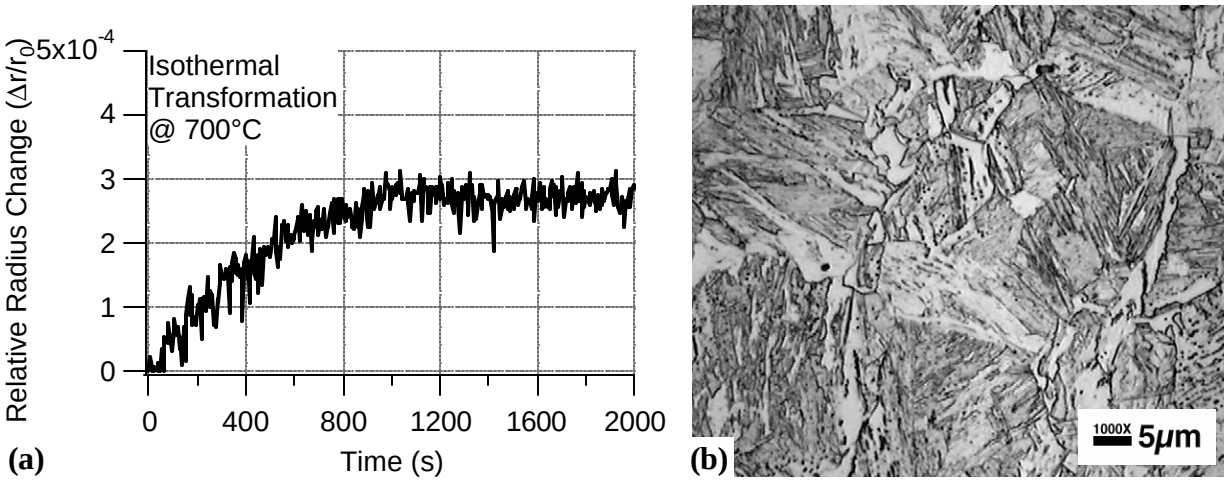

Figure 11. Preliminary experimental results on Fe-3Mn-0.1C held at 700°C after austenitization treatment. (a) Dilatation test results showing positive radius change with increasing time, indicative of partial austenite to ferrite transformation and (b) corresponding optical micrograph of sample after 30 minutes showing some proeutectoid ferrite (light, blocky phase) at prior austenite grain boundaries.

since the alloy composition lies outside the range in which LENP can take place. However, there are some discrepancies between the experimental results and the simulations presented earlier. First, the simulations predict the transformation to ferrite under para-equilibrium conditions will result in 72 vol % ferrite, and this level is far above that observed experimentally. Second, the simulations predict the transformation will reach completion within approximately 300 s but the experimental data show the transformation is still taking place after 1000 s. Further study, including metallography, will hopefully shed some light on these discrepancies. One explanation is that the para-equilibrium transformation temperature as predicted by computational thermodynamics is in error. If the para-equilibrium transformation temperature is significantly lower than 740°C, which if the value predicted by computational thermodynamics, then the fraction of ferrite formed will be less and the transformation kinetics will be slowed since close to the transformation temperature one lies above the nose of the TTT transformation curve [8]. The hypothesis that the transformation temperature is overpredicted by computational thermodynamics is supported in two ways. First, additional tests run at 730°C following austenitization did not show any sign of ferrite formation, indicating that this is above the para-equilibrium transformation temperature. Second, calculations using the quasi-chemical approach for evaluating para-equilibrium [8-10] showed the transformation temperature was close to 717°C. Another explanation is that nucleation of ferrite must be taken into account. If the nucleation barrier is not negligible, then both the transformation temperature and transformation rate will be reduced compared to the simulation calculation. The transformation rate will also be affected by the cell size used in the simulations, and a smaller cell size could yield a slower transformation rate because impingement effects would come into play earlier. Finally, an alternative transformation mechanism may be responsible for the discrepancies. A solute drag model could explain the present results. In fact, similar results were found by Oi et al [11], where the extent and rate of ferrite formation were found to be less than that expected under para-equilibrium conditions and the results were interpreted in terms of a solute drag model. Further experimental work is planned to clarify the transformation kinetics and to determine whether ferrite reversion takes place at longer hold times.

Conclusions

Results from simulations of the austenite to ferrite transformation using computational thermodynamics and kinetics models have been presented. The results show that if a condition

of para-equilibrium is imposed at the moving interface, followed by ortho-equilibrium at later stages, a unique transient ferrite dissolution stage is predicted. This stage is well-explained by considering the fluxes at the interface, and is absent under ortho-equilibrium interface conditions, including LENP conditions. Early experimental results show some limited ferrite formation is found within the same time frame predicted by the para-equilibrium condition. The rapid initial ferrite formation cannot be explained by ortho-equilibrium behavior or LENP transformation behavior.

Acknowledgments

This research was sponsored by the Division of Materials Sciences and Engineering, U. S. Department of Energy, under contract DE-AC05-00OR22725 with UT-Battelle, LLC. The authors would also like to thank Prof. W. T. Reynolds, Jr. Of Virginia Polytechnic University for supplying the materials used in the experimental work. Financial support for EK by the Austrian Kplus program is gratefully acknowledged.

References

1. M. Hillert, *Phase Equilibria, Phase Diagrams and Phase Transformations - Their Thermodynamic Basis* (New York, NY: Cambridge University Press, 1998), 348-367.
2. G. Inden, "Computational Thermodynamics and Simulation of Phase Transformations," *CALPHAD and Alloy Thermodynamics*, eds. P. E. A. Turchi, A. Gonis and R. D. Shull (Warrendale, PA: TMS, 2002), 107-130.
3. E. Kozeschnik, "A Discussion of Phase Transformations in Fe-C-Mn as Affected by Paraequilibrium Constraints." *J. Phase Equil.*, 21 (2000), 336-341.
4. B. Sundman, B. Jansson and J.-O. Andersson, "The ThermoCalc Databank System," *Calphad*, 9 (1985), 153-190.
5. E. Kozeschnik and B. Buchmayr, "MatCalc - A Simulation Tool for Multicomponent Thermodynamics, Diffusion and Phase Transformation Kinetics," *Mathematical Modelling of Weld Phenomena 5*, ed. H. Cerjak (London: Inst. of Materials, 2001), 349-361.
6. SGTE Solution Database (1992) Editor: B Sundman, Division of Computational Thermodynamics, Royal Institute of Technology, Stockholm, Sweden.
7. J.-O. Andersson, L. Höglund, B. Jönsson and J. Ågren, "Computer Simulation of Multicomponent Diffusional Transformations in Steel," *Fundamentals and Applications of Ternary Diffusion*, ed. G. R. Purdy (New York, NY: Pergamon Press, 1990), 153-163.
8. H. K. D. H. Bhadeshia, "A Thermodynamic Analysis of Isothermal Transformation Diagrams," *Metal Sci.*, 16 (1982), 159-165.
9. H. I. Aaronson, H. A. Domain and G. M. Pound, "Thermodynamics of the Austenite → Proeutectoid Ferrite Transformation II. Fe-C-X Alloys," *Trans. Met. Soc. AIME*, 236 (1966), 768-781.
10. G. J. Shiflet, J. R. Bradley and H. I. Aaronson, "A Re-examination of the Proeutectoid Ferrite Transformation in Fe-C Alloys," *Metall. Trans. A*, 9A (1978), 999-1008.
11. K. Oi, C. Luxand and G. R. Purdy, "A Study of the Influence of Mn and Ni on the Kinetics of the Proeutectoid Ferrite Reaction in Steels," *Acta Mater.*, 48 (2000), 2147-2155.